

A GENERAL MODEL FOR THE NONLINEAR ANALYSIS OF BEAMS INCLUDING THE EFFECTS OF SECTION DISTORTIONS

Alessandra Genoese, Andrea Genoese, Antonio Bilotta, Giovanni Garcea*

Laboratorio di Meccanica Computazionale, DIMES,
Università della Calabria,
via P. Bucci, cubo 39C 87036 Rende (CS), Italy
*e-mail: giovanni.garcea@unical.it

Key words: nonuniform warpings, section distortions, composite beams, Koiter asymptotic approach

Abstract. A geometrically nonlinear beam model suitable for describing complex 3D effects due to non-uniform warpings including non-standard in-plane distortions of the cross-section is presented. Buckling analysis results are compared with reference solutions obtained using the commercial code ABAQUS on the bases of a shell finite elements discretization. The beam model is potentially extendible to the analysis of anisotropic and heterogeneous material.

1 INTRODUCTION

The use of 3D beams and frames in composite materials or thin-walled profiles is continuously increasing in engineering practice, requiring appropriate analysis tools, capable of accurately predicting complex 3D behaviours such as interlaminar stresses, section distortions and non-standard coupling effects. 3D solid or shell based analyses are computationally more expensive and the recourse to accurate 1D formulations, capable of reproducing the essential aspects of the original solution is then preferable. This is the case, for instance, of the generalized beam theory (GBT) initially proposed by Schardt [1] for modeling thin walled isotropic profiles and notably improved in the last few years principally by Camotim and coauthors (see [2, 3] among other works).

This work deals with the formulation of a geometrically nonlinear beam model suitable for describing non-uniform warpings effects including non-standard in-plane distortions of the cross-section and potentially to account in a natural way for other 3D effects. The work is limited to isotropic material but the formulation is general and, in our opinion, extendible to cases of beams with anisotropic and heterogeneous material. The basic idea of the proposal is that of extending the generalized beam model presented in [4] (see also

[5]) to the case of large displacements but small strains through the Implicit Corotational Method (ICM) proposed in [6]. ICM extends the corotational description at the continuum level by introducing a corotational reference system for each cross-section. In this system, following a mixed approach, the linear stress tensor is shown to be a good approximation of the Biot nonlinear one, while a quadratic approximation of the strain is easily obtained from the symmetric and the skew-symmetric parts of the displacement gradient of the parent linear solution. The two fields so defined are introduced in the Hellinger-Reissner functional to describe the beam behaviour in terms of generalized static and kinematic quantities only, while change of observer algebra is used to complete the framework. The nonlinear model maintains all the information of its linear counterpart, but is objective and accurate up to the required order. This feature makes it suitable to be used within both a standard incremental iterative approach or FEM implementations of the Koiter asymptotic method. Readers are referred to [7] for its first application to the Saint-Venant (SV) and the Kirchhoff solutions for beams and plates, while in references [8, 9] an extension to homogeneous and isotropic beams subjected to variable shear/torsion warping deformations is presented. The linear formulations used in [4, 5] have been proved to be very effective for modeling beams made of isotropic and homogeneous material or by composites, also when important warping effects including non-standard in-plane distortions of the cross-section arise (see [4] in particular). These models are defined exploiting a semi-analytical solution of the Cauchy continuum problem for beam-like bodies under the usual SV loading conditions, based on an FEM discretization of the cross-section (see also [10] for details). The stress field considered in this way is potentially fully 3D, allowing the recovery of SV solution for standard materials (see [11] for instance) or to generalize it to inhomogeneous and anisotropic cross-sections. Furthermore some additional relevant strain modes (generalized warpings) of the cross-section can be defined in a coherent and effective way. On the basis of this information, the 1D linear model is described in a mixed format as required by the ICM framework. As in [11], the displacement field is approximated in terms of a rigid section motion and other relevant generalized warping modes independently amplified along the beam axial direction. The stress field instead enriches that provided by the generalized SV solution through the contributions due to all the generalized warping effects considered. A mixed finite element suitable for interpolating both the kinematic and static generalized unknowns is proposed. It is implemented inside a Koiter-like asymptotic algorithm. Numerical results regarding the buckling loads evaluation are shown and compared with reference solutions obtained on the bases of shell finite elements which are more computationally expensive.

2 THE BEAM MODEL

2.1 The Linear Solution

Let us consider the beam as a Cauchy body referred to a fixed Cartesian frame with origin \mathcal{O} and basis vectors $\{\mathbf{e}_1, \mathbf{e}_2, \mathbf{e}_3\}$. Each material reference point is defined by a

position vector $\mathbf{X} = x_1 \mathbf{e}_1 + \mathbf{x}$, x_1 being a one-dimensional abscissa along the axis line or *support* of length ℓ while $\mathbf{x} = x_2 \mathbf{e}_2 + x_3 \mathbf{e}_3$ lies on the cross section or *fiber* $\Omega[x_1]$.

The linear solution in terms of displacement is assumed in the form

$$\bar{\mathbf{v}}[x_1, \mathbf{x}] = \bar{\mathbf{v}}_o[x_1] + \Theta[\mathbf{x}]^T \bar{\boldsymbol{\varphi}}[x_1] + \mathbf{A}_\omega[\mathbf{x}] \boldsymbol{\mu}[x_1] \quad (1)$$

where $\bar{\mathbf{v}}_o[x_1]$ and $\bar{\boldsymbol{\varphi}}[x_1]$ are suitable mean values of the translation and rotation of the section, $\Theta[\cdot] = \text{spin}(\cdot)$, while $\boldsymbol{\mu}[x_1]$ gives the variability, along the beam axis, of the most important n generalized warping functions $\boldsymbol{\omega}^{(i)}[\mathbf{x}]$ evaluated through the cross-section analysis proposed in [4] and collected in the matrix

$$\mathbf{A}_\omega[\mathbf{x}] = [\boldsymbol{\omega}^{(1)}[\mathbf{x}], \dots, \boldsymbol{\omega}^{(n)}[\mathbf{x}]]. \quad (2)$$

Let $\boldsymbol{\varepsilon}_L[x_1] = \bar{\mathbf{v}}_{o,1} + \Theta[\mathbf{e}_1] \bar{\boldsymbol{\varphi}}$ and $\boldsymbol{\chi}_L[x_1] = \bar{\boldsymbol{\varphi}}_{,1}$ be the standard generalized strains. Introducing vector $\boldsymbol{\rho}_L[x_1] = \{\boldsymbol{\varepsilon}_L, \boldsymbol{\chi}_L, \boldsymbol{\mu}_{,1}, \boldsymbol{\mu}\}$ and matrices

$$\mathbf{U}_1[\mathbf{x}] = [\mathbf{I}, \Theta[\mathbf{x}]^T, \mathbf{A}_\omega, \mathbf{0}], \quad \mathbf{U}_2[\mathbf{x}] = [\mathbf{0}, \mathbf{0}, \mathbf{0}, \mathbf{A}_{\omega,2}], \quad \mathbf{U}_3[\mathbf{x}] = [\mathbf{0}, \mathbf{0}, \mathbf{0}, \mathbf{A}_{\omega,3}]$$

the displacement gradient is

$$\nabla \bar{\mathbf{v}} = [\bar{\mathbf{v}}_{,1} \quad \bar{\mathbf{v}}_{,2} \quad \bar{\mathbf{v}}_{,3}], \quad \bar{\mathbf{v}}_{,k} = \mathbf{U}_k[\mathbf{x}] \boldsymbol{\rho}_L[x_1] \quad (3)$$

Introducing $\mathbf{s}[x_1, \mathbf{x}] = \{\sigma_{11}, \sigma_{12}, \sigma_{13}\}$ and $\mathbf{r}[x_1, \mathbf{x}] = \{\sigma_{22}, \sigma_{33}, \sigma_{23}\}$, the stress components in $\boldsymbol{\sigma}[x_1, \mathbf{x}] = \{\mathbf{s}, \mathbf{r}\}$ are evaluated as

$$\boldsymbol{\sigma} = \mathbf{D}_\sigma[\mathbf{x}] \mathbf{t}[x_1], \quad (4)$$

where $\mathbf{t}[x_1] = \{\mathcal{N}, \mathcal{M}, \mathcal{B}, \mathcal{T}\}$ collects the resultant forces $\mathcal{N} = \int_\Omega \mathbf{s}$ and moments $\mathcal{M} = \int_\Omega \Theta[\mathbf{x}] \mathbf{s}$ the n bimoments in \mathcal{B} and bishears in \mathcal{T} , while

$$\mathbf{D}_\sigma[\mathbf{x}] = [\mathbf{d}^{(N_1)}, \dots, \mathbf{d}^{(N_3)}, \mathbf{d}^{(M_1)}, \dots, \mathbf{d}^{(M_3)}, \mathbf{d}^{(\mathcal{B}_1)}, \dots, \mathbf{d}^{(\mathcal{B}_n)}, \mathbf{d}^{(\mathcal{T}_1)}, \dots, \mathbf{d}^{(\mathcal{T}_n)}]$$

with the 6 components of each vector $\mathbf{d}^{(\alpha)}$ explicitly defined in [4]. We only recall that they depend on the n generalized warpings $\boldsymbol{\omega}^{(i)}$ and a central solution coincident with the SV one for isotropic and homogeneous materials. They are defined by an eigenproblem over the section which reduces to 8 linear systems with the same iteration matrix (see also [10]) for the central part of the solution.

Finally, introducing the operator $\mathbf{D}_\omega = \mathbf{D} \mathbf{A}_\omega$ with

$$\mathbf{D} = \begin{bmatrix} \mathbf{D}_e \\ \mathbf{D}_g \end{bmatrix}, \quad \mathbf{D}_e = \begin{bmatrix} 0 & 0 & 0 \\ \frac{\partial}{\partial x_2} & 0 & 0 \\ \frac{\partial}{\partial x_3} & 0 & 0 \end{bmatrix}, \quad \mathbf{D}_g = \begin{bmatrix} 0 & \frac{\partial}{\partial x_2} & 0 \\ 0 & 0 & \frac{\partial}{\partial x_3} \\ 0 & \frac{\partial}{\partial x_3} & \frac{\partial}{\partial x_2} \end{bmatrix}$$

bimoments and bishears are defined as $\mathcal{B} = \int_\Omega \mathbf{A}_\omega^T \mathbf{s}$ and $\mathcal{T} = \int_\Omega \mathbf{D}_\omega^T \boldsymbol{\sigma}$.

2.2 The extention to the nonlinear case

We introduce for each fiber a corotational observer defined by the mean translation \mathbf{v}_o and rotation $\mathbf{R}[x_1]$. In this system the displacement gradient components are evaluated using the linear solution (3), where $\bar{\boldsymbol{\varphi}} = \mathbf{0}$. From now on the bar will denote the corotational quantities.

In the following we will adopt the vector-like parametrization of the 3D rotations, introduced by Rodrigues and largely used in finite element analysis. Generalized strains $\boldsymbol{\varepsilon}_L$ and $\boldsymbol{\chi}_L$ can then be related to displacements \mathbf{v}_o with respect to a fixed reference system and the rotation vector $\boldsymbol{\varphi}$ using a standard change of observer algebra as

$$\boldsymbol{\varepsilon}_L[x_1] = \mathbf{R}[\boldsymbol{\varphi}]^T(\mathbf{v}_{0,1} + \mathbf{e}_1) - \mathbf{e}_1, \quad \boldsymbol{\chi}_L[x_1] = \boldsymbol{\Lambda}[\boldsymbol{\varphi}]^T \boldsymbol{\varphi}_{,1}. \quad (5)$$

where

$$\mathbf{R} = \sum_{k=0}^{\infty} \frac{\boldsymbol{\Theta}[\boldsymbol{\varphi}]^k}{k!} = \mathbf{I} + \boldsymbol{\Theta}[\boldsymbol{\varphi}] + \frac{1}{2}\boldsymbol{\Theta}[\boldsymbol{\varphi}]^2 + \dots, \quad \boldsymbol{\Lambda} = \sum_{k=0}^{\infty} \frac{\boldsymbol{\Theta}[\boldsymbol{\varphi}]^k}{(k+1)!} = \mathbf{I} + \frac{1}{2}\boldsymbol{\Theta}[\boldsymbol{\varphi}] + \frac{1}{6}\boldsymbol{\Theta}[\boldsymbol{\varphi}]^2 + \dots.$$

The warping parameters $\boldsymbol{\mu}$ as the static part of the solution do not require any changes of observer algebra.

With the same Voigt notation used for stresses, Biot strains are collected in $\boldsymbol{\varepsilon}[x_1, \mathbf{x}] = \{\mathbf{e}, \mathbf{g}\}$, with $\mathbf{e}[x_1, \mathbf{x}] = \{\varepsilon_{11}, \gamma_{12}, \gamma_{13}\}$ and $\mathbf{g}[x_1, \mathbf{x}] = \{\varepsilon_{22}, \varepsilon_{33}, \gamma_{23}\}$. Referring to [6] for a deeper discussion, strains components in $\boldsymbol{\varepsilon}$ are evaluated in terms of the displacement gradient as

$$\varepsilon_i = \mathbf{L}_i[\mathbf{x}] \boldsymbol{\rho}_L[x_1] + \frac{1}{2} \boldsymbol{\rho}_L^T[x_1] \mathbf{B}_i[\mathbf{x}] \boldsymbol{\rho}_L[x_1] \quad (6)$$

where operators \mathbf{L}_i and \mathbf{B}_i are defined introducing $\mathbf{I}_{ij} = \mathbf{e}_i \mathbf{e}_j^T$ and matrices

$$\mathbf{L}_{ij}[\mathbf{x}] = \frac{1}{2}(\mathbf{e}_i^T \mathbf{U}_j + \mathbf{e}_j^T \mathbf{U}_i), \quad \mathbf{B}_{ij}[\mathbf{x}] = \frac{3}{4} \mathbf{U}_i^T \mathbf{U}_j - \frac{1}{4} \sum_{k=1}^3 (\mathbf{U}_j^T \mathbf{I}_{ki} \mathbf{U}_k + \mathbf{U}_i^T \mathbf{I}_{kj} \mathbf{U}_k + \mathbf{U}_k^T \mathbf{I}_{ij} \mathbf{U}_k)$$

which allow us to write

$$\varepsilon_{ij} = \mathbf{L}_{ij}[\mathbf{x}] \boldsymbol{\rho}_L[x_1] + \frac{1}{2} \boldsymbol{\rho}_L^T[x_1] \mathbf{B}_{ij}[\mathbf{x}] \boldsymbol{\rho}_L[x_1].$$

We have then, for instance, $\mathbf{L}_1 = \mathbf{L}_{11}$, $\mathbf{L}_2 = \mathbf{L}_{12} + \mathbf{L}_{21}$, $\mathbf{B}_1 = \mathbf{B}_{11}$, $\mathbf{B}_2 = \mathbf{B}_{12} + \mathbf{B}_{21}$ and so on.

The nonlinear beam model is derived as a Ritz-Galerkin approximation introducing the static and kinematic fields previously evaluated in the Hellinger-Reissner functional

$$\Pi_{HR} \equiv \mathcal{W} - \Psi - \mathcal{L}$$

where \mathcal{L} is the contribution of the external work, \mathcal{W} is the stress strain work and Ψ the complementary energy contribution. Denoting as \mathbf{F} the elastic compliance operator, we have

$$\Psi = \frac{1}{2} \int_{\ell} \int_{\Omega} \boldsymbol{\sigma}^T \mathbf{F} \boldsymbol{\sigma} = \frac{1}{2} \int_{\ell} \mathbf{t}^T \mathbf{H} \mathbf{t}, \quad (7)$$

where $\mathbf{H} = \int_{\Omega} \mathbf{D}_{\sigma}^T \mathbf{F} \mathbf{D}_{\sigma}$ is the cross-section flexibility matrix.

Finally, the stress strain work is defined as

$$\mathcal{W} = \int_{\ell} \int_{\Omega} \boldsymbol{\sigma}^T \boldsymbol{\varepsilon} = \int_{\ell} \mathbf{t}^T (\boldsymbol{\rho}_L + \boldsymbol{\rho}_Q[\boldsymbol{\rho}_L, \boldsymbol{\rho}_L]), \quad (8)$$

where $\boldsymbol{\rho}_Q = \{\rho_Q^{(N_1)}, \dots, \rho_Q^{(N_3)}, \rho_Q^{(M_1)}, \dots, \rho_Q^{(M_3)}, \rho_Q^{(B_1)}, \dots, \rho_Q^{(B_n)}, \rho_Q^{(T_1)}, \dots, \rho_Q^{(T_n)}\}$ with

$$\rho_Q^{(\alpha)} = \frac{1}{2} \boldsymbol{\rho}_L^T \boldsymbol{\Upsilon}^{(\alpha)} \boldsymbol{\rho}_L, \quad \boldsymbol{\Upsilon}^{(\alpha)} = \sum_{i=1}^6 \int_{\Omega} d_i^{(\alpha)} \mathbf{B}_i. \quad (9)$$

3 THE BUCKLING ANALYSIS

In the following the buckling analysis is considered as the first step of a complete asymptotic Koiter FE analysis, described in detail in [12, 13, 14, 15, 16].

We consider a slender hyperelastic structure subjected to conservative loads $\lambda \hat{\mathbf{p}}$ linearly increasing with the amplifier factor λ . The equilibrium is expressed by the virtual work equation:

$$\Phi'[u] \delta u - \lambda \hat{\mathbf{p}} \delta u = 0, \quad \forall \delta u \in \mathcal{T} \quad (10)$$

where $u \in \mathcal{U}$ is the field of configuration variables, $\Phi[u]$ denotes the strain energy, \mathcal{T} is the tangent space of \mathcal{U} at u and a prime is used for expressing the Fréchet derivative with respect to u . We assume that \mathcal{U} will be a linear manifold so that its tangent space \mathcal{T} will be independent from u .

From now on we consider a FEM interpolation so that symbol in bold will denote the vector collecting displacements and the stress finite element parameters while the corresponding continuous quantities will be denoted with symbols not in bold. The solution algorithm for the buckling analysis requires, from a computational point of view, the following steps

1. *the fundamental path* is described by means of the linear extrapolation $u^f[\lambda] = \lambda \hat{u}$, where the initial path tangent \hat{u} is obtained as the solution of the linear vectorial equation

$$\mathbf{K}_0 \hat{\mathbf{u}} = \hat{\mathbf{p}}, \quad \Phi_0'' \hat{\mathbf{u}} \delta u = \delta \mathbf{u}^T \mathbf{K}_0 \hat{\mathbf{u}}, \quad \forall \delta u \in \mathcal{T} \quad (11)$$

$\hat{\mathbf{p}}$ being the discrete load vector and \mathbf{K}_0 the stiffness matrix evaluated for $\lambda = 0$, i.e. $\Phi_0'' = \Phi''[u^f[\lambda = 0]]$;

2. a cluster of *buckling loads* and *modes* $\{\lambda_i, \dot{\mathbf{v}}_i\}$, $i = 1 \dots m$, is obtained along $\mathbf{u}^f[\lambda]$, by exploiting the critical condition

$$\mathbf{K}[\lambda_i] \dot{\mathbf{v}}_i = \mathbf{0}, \quad (12)$$

the tangent stiffness matrix $\mathbf{K}[\lambda]$ being defined by the equivalence $\mathbf{u}_i^T \mathbf{K}[\lambda] \mathbf{u}_j = \Phi''[\lambda \hat{u}] u_i u_j$.

3.1 The tangent stiffness matrix

The element tangent stiffness matrix will be derived by using a linearization in the origin of Eq.(12)

$$\Phi''[\lambda \hat{u}] u_i u_j \approx (\Phi''_0 + \lambda \Phi'''_0 \hat{u}) u_i u_j, \quad \mathbf{K}[\lambda] \dot{\mathbf{v}}_i \approx (\mathbf{K}_0 + \lambda \hat{\mathbf{K}}_0) \dot{\mathbf{v}}_i = \mathbf{0} \quad (13)$$

where u_k represents a generic variation of u and a subscript zero denotes quantity evaluated for $\lambda = 0$.

Denoting as \mathbf{d}_k and \mathbf{t}_k a generic variation of $\mathbf{d} = \{\mathbf{v}_{o,1}, \boldsymbol{\varphi}, \boldsymbol{\varphi}_{,1}, \boldsymbol{\mu}, \boldsymbol{\mu}_{,s}\}$ and \mathbf{t} , we obtain

$$\Phi''[\lambda \hat{u}] u_i u_j \approx \int_{\ell} \mathbf{t}_i^T \boldsymbol{\rho}'_L[\mathbf{d}_j] + \mathbf{t}_j^T \boldsymbol{\rho}'_L[\mathbf{d}_i] - \mathbf{t}_i^T \mathbf{H} \mathbf{t}_j + \lambda \hat{\mathbf{t}}^T \boldsymbol{\rho}''[\mathbf{d}_i, \mathbf{d}_j] \quad (14)$$

where $\boldsymbol{\rho}'_L[\mathbf{d}_i] = \{\boldsymbol{\varepsilon}'_L[\mathbf{d}_i], \boldsymbol{\chi}'_L[\mathbf{d}_i], \boldsymbol{\mu}'_{,s}[\mathbf{d}_i], \boldsymbol{\mu}'[\mathbf{d}_i]\}$, while, introducing $\mathbf{G}[\hat{\mathbf{t}}] = \sum_{\alpha} \hat{t}^{(\alpha)} \boldsymbol{\Upsilon}^{(\alpha)}$,

$$\boldsymbol{\rho}''[\mathbf{d}_i, \mathbf{d}_j] = \boldsymbol{\rho}''_L[\mathbf{d}_i, \mathbf{d}_j] + \boldsymbol{\rho}'_L[\mathbf{d}_i]^T \mathbf{G}[\hat{\mathbf{t}}] \boldsymbol{\rho}'_L[\mathbf{d}_j],$$

with $\boldsymbol{\rho}''_L[\mathbf{d}_i, \mathbf{d}_j] = \{\boldsymbol{\varepsilon}''_L[\mathbf{d}_i, \mathbf{d}_j], \boldsymbol{\chi}''_L[\mathbf{d}_i, \mathbf{d}_j], \mathbf{0}, \mathbf{0}\}$. Note as in Eq. (14) displacement quantities $\lambda \hat{\mathbf{d}}$ have been neglected.

Defining $\mathbf{V}_2[\mathbf{a}, \mathbf{b}] = \boldsymbol{\Theta}[\mathbf{a}] \boldsymbol{\Theta}[\mathbf{b}] + \boldsymbol{\Theta}[\mathbf{b}] \boldsymbol{\Theta}[\mathbf{a}]$, we obtain from Eq. (5)

$$\begin{aligned} \boldsymbol{\varepsilon}'_L[\mathbf{d}_i] &= \mathbf{v}_{oi,1} + \boldsymbol{\Theta}[\mathbf{e}_1] \boldsymbol{\varphi}_i, & \boldsymbol{\varepsilon}''_L[\mathbf{d}_j, \mathbf{d}_i] &= -(\boldsymbol{\Theta}[\boldsymbol{\varphi}_j] \mathbf{v}_{oi,1} + \boldsymbol{\Theta}[\boldsymbol{\varphi}_i] \mathbf{v}_{oj,1}) + \frac{1}{2} \mathbf{V}_2[\boldsymbol{\varphi}_i, \boldsymbol{\varphi}_j] \mathbf{e}_1, \\ \boldsymbol{\chi}'_L[\mathbf{d}_i] &= \boldsymbol{\varphi}_{i,1}, & \boldsymbol{\chi}''_L[\mathbf{d}_i, \mathbf{d}_j] &= -\frac{1}{2} (\boldsymbol{\Theta}[\boldsymbol{\varphi}_j] \boldsymbol{\varphi}_{i,1} + \boldsymbol{\Theta}[\boldsymbol{\varphi}_i] \boldsymbol{\varphi}_{j,1}). \end{aligned} \quad (15)$$

Introducing $\mathbf{u}[x_1] = \{\mathbf{t}, \mathbf{d}\}$ and $\mathbf{u}_e = \{\boldsymbol{\beta}_e, \mathbf{q}_e\}$ collecting all the finite element parameters, the interpolation can be written as

$$\mathbf{u}[x_1] = \mathbf{N}_u[x_1] \mathbf{u}_e \quad \mathbf{N}_u = \begin{bmatrix} \mathbf{N}_t[x_1] & \cdot \\ \cdot & \mathbf{N}_d[x_1] \end{bmatrix}.$$

We can then define the tangent stiffness matrix $\mathbf{K}_e[\lambda]$ as

$$\Phi'' u_i u_j = \mathbf{u}_{ei}^T \mathbf{K}_e[\lambda] \mathbf{u}_{ej}, \quad \mathbf{K}_e[\lambda] = \int_{\ell} \mathbf{N}_u^T \mathbf{K}[\lambda] \mathbf{N}_u. \quad (16)$$

Introducing the identity matrix of order m \mathbf{I}_m , terms in

$$\mathbf{K}[\lambda] = \begin{bmatrix} -\mathbf{H} & \mathbf{K}_{td} \\ \mathbf{K}_{td}^T & \lambda \mathbf{K}_{dd} \end{bmatrix}$$

are defined as

$$\mathbf{K}_{td} = \begin{bmatrix} \mathbf{I}_3 & \Theta[\mathbf{e}_1] & \cdot & \cdot & \cdot \\ \cdot & \cdot & \mathbf{I}_3 & \cdot & \cdot \\ \cdot & \cdot & \cdot & \cdot & \mathbf{I}_n \\ \cdot & \cdot & \cdot & \mathbf{I}_n & \cdot \end{bmatrix}, \quad \mathbf{K}_{dd}[\hat{\mathbf{t}}] = \mathbf{K}_{dd}^{(L)}[\hat{\mathbf{t}}] + \mathbf{K}_{dd}^{(Q)}[\hat{\mathbf{t}}]$$

with

$$\mathbf{K}_{dd}^{(L)} = \begin{bmatrix} \cdot & -\Theta[\hat{\mathcal{N}}] & \cdot & \cdot & \cdot \\ \Theta[\hat{\mathcal{N}}] & \frac{1}{2}\mathbf{V}_2[\hat{\mathcal{N}}, \mathbf{e}_1] & \frac{1}{2}\Theta[\hat{\mathcal{M}}] & \cdot & \cdot \\ \cdot & -\frac{1}{2}\Theta[\hat{\mathcal{M}}] & \cdot & \cdot & \cdot \\ \cdot & \cdot & \cdot & \cdot & \cdot \\ \cdot & \cdot & \cdot & \cdot & \cdot \end{bmatrix}, \quad \mathbf{K}_{dd}^{(Q)} = \mathbf{K}_{td}^T \mathbf{G}[\hat{\mathbf{t}}] \mathbf{K}_{td}.$$

We refer to [9] for the explicit expression of shape functions used to interpolate $\mathbf{v}_{o,s}$, φ , \mathcal{N} and \mathcal{M} . Note as with respect to [9], cubic lagrangian polynomials are adopted for the warping descriptors $\boldsymbol{\mu}$, while \mathcal{B} and \mathcal{T} are described through separate quadratic interpolations. Finally integration of the quantities on the element can be easily performed by means of a Gauss point numeric process.

4 NUMERICAL RESULTS

Let us consider the simply supported beam with channel section in Figure 1, already proposed in [13]. The structure is subjected to an axial compression uniform over the cross-section and to a system of two local forces at midspan, uniformly applied over the channel wedges (we refer to [4] for the load equivalence on the beam).

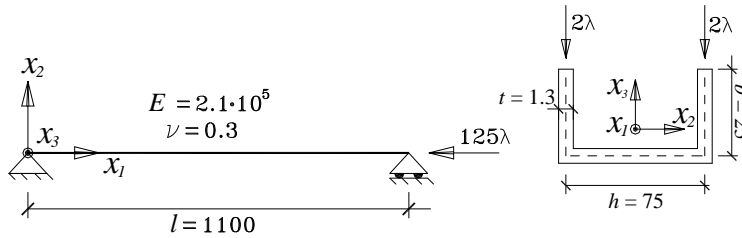


Figure 1: Simply supported beam with channel section

The analysis is performed considering a variable number of generalized warping modes from 0 to 13 + 13 (13 with only in-plane displacement components and 13 with only that

in the beam axial direction). The first 18 of these modes are depicted in Figures 2 and 3. For the one-dimensional solution a mesh of 4 and 32 FEs is considered, respectively, for the case of 0 additional warping modes and for the other cases.

Table 1 shows a comparison between values of the smallest 6 buckling loads obtained with our proposal and those furnished by a shell modeling performed with the commercial code *ABAQUS* using a mesh of $(3 + 9 + 3) \times 60$ *S8R* FEs. In-plane generalized warpings are prevented at the beam ends as for the torsional rotation and the lateral displacements while the axial displacement u_1 is prevented at only one side. The constraints used for the shell model are the same as described in [13].

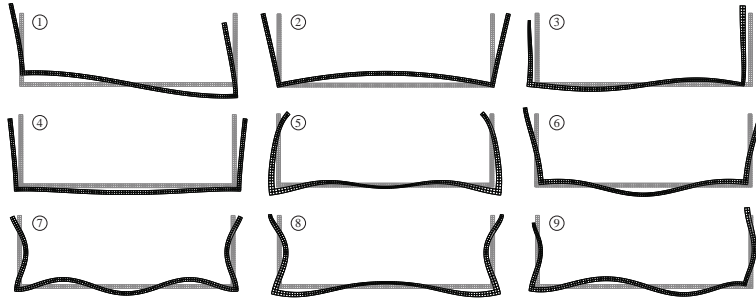


Figure 2: Simply supported beam with channel section: in-plane generalized warping modes

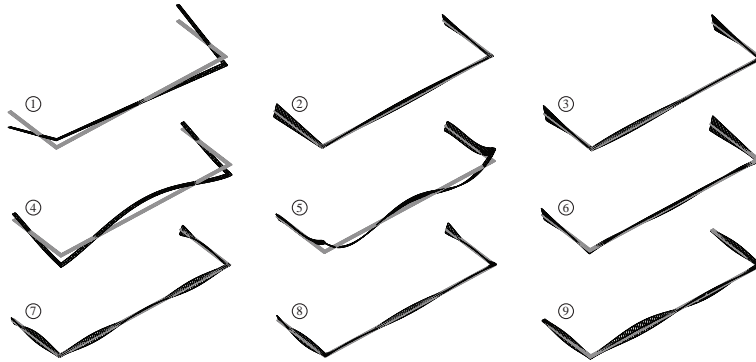


Figure 3: Simply supported beam with channel section: out-of-plane generalized warping modes

Figure 4 shows the buckling modes obtained (on the left) and those furnished by the *ABAQUS* shell analysis (on the right). Note the capability of the general beam formulation to accurately predict the local in-plane distortions.

Figures 5-7 report the significant warping parameters along the beam axis for the first 3 buckling modes. The localization of the μ -distributions is manifest in the central part of the beam because of the presence of the vertical force for the local mode.

modes	0	1	3	6	9	13	ABAQUS
λ_1	437.23	1293.8	1293.9	1296.6	1295.0	1295.0	1269.5
λ_2	472.62	1351.1	1331.9	1333.1	1327.7	1326.7	1291.4
λ_3	499.73	3957.6	2525.0	2306.8	2056.1	1986.2	1949.1
λ_4	542.43	5084.6	2573.4	2528.2	2065.8	1994.8	1961.8
λ_5	559.43	8753.3	2714.3	2528.4	2225.1	2160.4	2089.1
λ_6	636.11	11119	2737.2	2561.9	2228.7	2162.3	2096.4

Table 1: Simply supported beam with channel section: buckling loads

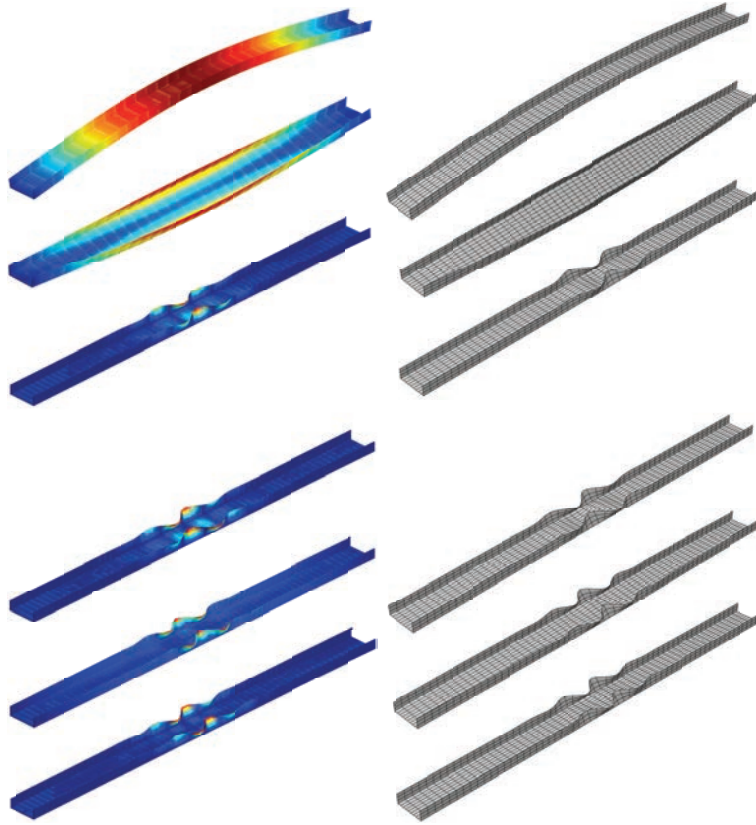


Figure 4: Simply supported beam with channel section: buckling modes

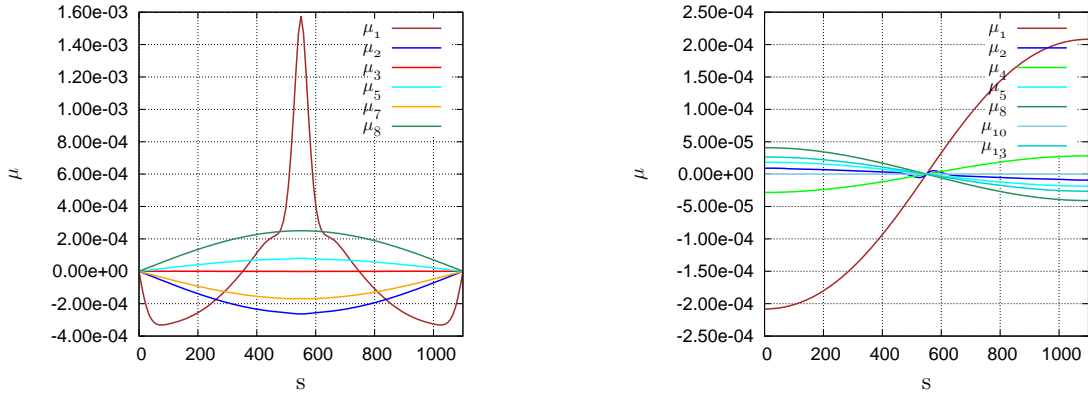


Figure 5: Simply supported C-shaped beam under compression and flexural imperfection: in-plane (left) and out-plane (right) μ distributions (most significant only) along the beam for the buckling mode 1.

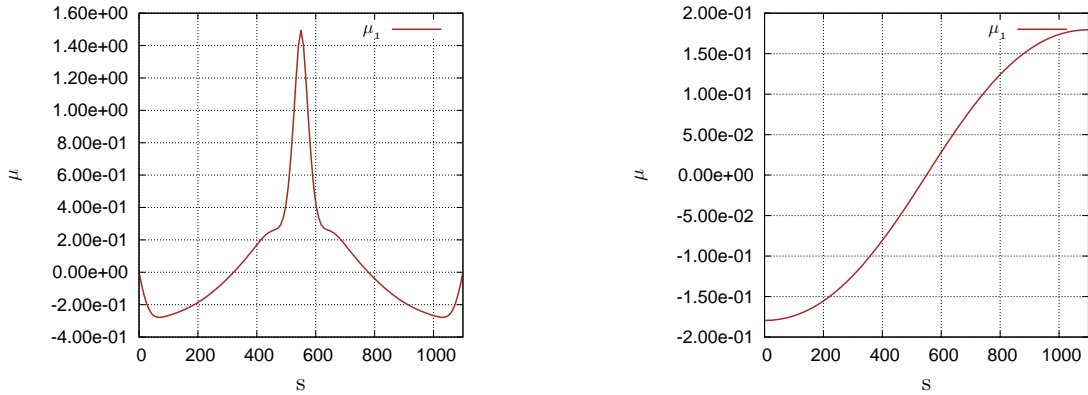


Figure 6: Simply supported C-shaped beam under compression and flexural imperfection: in-plane (left) and out-plane (right) μ distributions (most significant only) along the beam for the buckling mode 2.

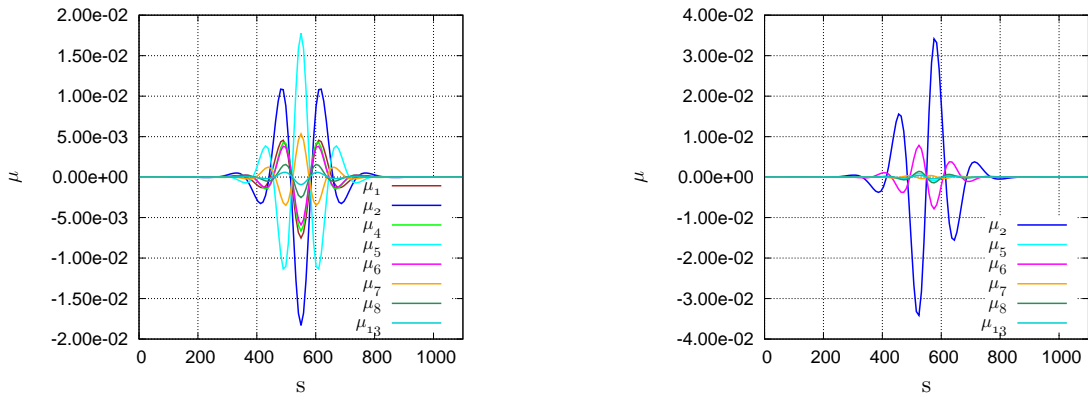


Figure 7: Simply supported C-shaped beam under compression and flexural imperfection: in-plane (left) and out-plane (right) μ distributions (most significant only) along the beam for the buckling mode 3.

5 CONCLUSIONS

In this work, the Implicit Corotational technique is employed to recover a nonlinear model for beams in space with variable warping effects including in-plane distortions of the cross-section, subjected to small strains but large displacements and rotations.

The numerical experimentation performed regarding the buckling analysis demonstrates the reliability and the accuracy of the formulation and its FEM reduction through comparisons with 3D shell-models.

REFERENCES

- [1] Schardt, R., Generalized beam theory-an adequate method for coupled stability problems, *Thin Wall. Struct.* (1984) **19** (2–4): 161–180.
- [2] Silvestre, N. and Camotim, D., On the mechanics of distortion in thin-walled open sections, *Thin Wall. Struct.* (2010) **48**: 469–481.
- [3] Camotim, D. and Basaglia, C. and Silvestre, N., GBT buckling analysis of thin-walled steel frames: A state-of-the-art report, *Thin Wall. Struct.*(2010) **48** (10–11): 726–743.
- [4] Genoese, A. and Genoese, A. and Bilotta, A. and Garcea G., A generalized model for heterogeneous and anisotropic beams including section distortions, *Thin Wall. Struct.* (2014) **74**: 85–103.
- [5] Genoese, A. and Genoese, A. and Bilotta, A. and Garcea G., A composite beam model including variable warping effects derived from a generalized Saint Venant solution, *Compos. Struct.* (2014) **110**: 140–151.
- [6] Garcea, G. and Madeo, A. and Casciaro R., The Implicit Corotational Method and its use in the derivation of nonlinear structural models for beam and plates, *J. Mech. Mater. Struct.* (2012) **7** (6): 509–539.
- [7] Garcea, G. and Madeo, A. and Casciaro R., Nonlinear FEM analysis for beams and plate assemblages based on the Implicit Corotational Method, *J. Mech. Mater. Struct.* (2012) **7** (6): 539-574.
- [8] Genoese, A. and Genoese, A. and Bilotta, A. and Garcea G., A general model for the analysis of beams including warping effects, *Proceedings XIV International Conference on Civil, Structural and Environmental Engineering Computing* (2013).
- [9] Genoese, A. and Genoese, A. and Bilotta, A. and Garcea G., A geometrically exact beam model with nonuniform warping coherently derived from the Saint Venant rod, *Eng. Struct.* (2014), **68C**: pp. 33-46.

- [10] Morandini, M. and Chierichetti, M. and Mantegazza, P., Characteristic behavior of prismatic anisotropic beams via generalized eigenvectors, *Int. J. Solids Struct.* (2010) **47 (10)**: 1327–1337.
- [11] Genoese, A. and Genoese, A. and Bilotta, A. and Garcea G., A mixed beam model with non-uniform warpings derived from the Saint Venant rod, *Comput. Struct.* (2013) **121**: 87–98.
- [12] Garcea, G. and Trunfio, G. A. and Casciaro, R., Mixed formulation and locking in path-following nonlinear analysis, *Comput. Method Appl. M.* (1998) **165 (1–4)**: 247–272.
- [13] Garcea, G., Mixed formulation in Koiter analysis of thin-walled beams, *Comput. Method Appl. M.* (2001) **190 (26–27)**: 3369-3399.
- [14] Lanzo, A.D. and Garcea, G. and Casciaro, R. Asymptotic post-buckling analysis of rectangular plates by HC finite elements, *Int. J. Numer. Meth. Eng.* (1995) **38 (14)**: 2325–2345.
- [15] Lanzo, A.D. and Garcea, G., Koiter’s analysis of thin-walled structures by a finite element approach, *Int. J. Numer. Meth. Eng.* (1996) **39 (17)**: 3007–3031.
- [16] Casciaro, R. and Garcea, G. and Attanasio, G. and Giordano, F., Perturbation approach to elastic post-buckling analysis, *Comput. Struct.* (1998) **66 (5)**: 585–595.